

## A formalism for calculating the modal contributions to thermal interface conductance

This content has been downloaded from IOPscience. Please scroll down to see the full text.

2015 New J. Phys. 17 103002

(<http://iopscience.iop.org/1367-2630/17/10/103002>)

View [the table of contents for this issue](#), or go to the [journal homepage](#) for more

Download details:

IP Address: 143.215.20.112

This content was downloaded on 12/12/2015 at 04:19

Please note that [terms and conditions apply](#).



## PAPER

## A formalism for calculating the modal contributions to thermal interface conductance

## OPEN ACCESS

## RECEIVED

2 May 2015

## REVISED

31 August 2015

## ACCEPTED FOR PUBLICATION

7 September 2015

## PUBLISHED

30 September 2015

Content from this work  
may be used under the  
terms of the [Creative  
Commons Attribution 3.0  
licence](#).

Any further distribution of  
this work must maintain  
attribution to the  
author(s) and the title of  
the work, journal citation  
and DOI.

Kiarash Gordiz<sup>1</sup> and Asegun Henry<sup>1,2</sup><sup>1</sup> George W Woodruff School of Mechanical Engineering, Georgia Institute of Technology, Atlanta GA 30332, USA<sup>2</sup> School of Materials Science and Engineering, Georgia Institute of Technology, Atlanta GA 30332, USAE-mail: [ase@gatech.edu](mailto:ase@gatech.edu)**Keywords:** thermal interface conductance, modal decomposition, molecular dynamicsSupplementary material for this article is available [online](#)**Abstract**

A formalism termed the interface conductance modal analysis (ICMA) method is presented, which allows for calculations of the modal contributions to thermal interface conductance within the context of molecular dynamics (MD) simulations, which inherently include anharmonicity to full order. The eigen modes of vibration in this study are calculated from harmonic lattice dynamics (LD) calculations, however the generality of ICMA formalism also allows for incorporation of anharmonic LD results into the calculations. ICMA can be implemented in both equilibrium MD (EMD) and non-equilibrium MD (NEMD) simulations and both methods show qualitative agreement as validated through study of a simple system of Lennard-Jones solids. The formalism itself is based on a modal decomposition of the heat flow across an interface, which is then substituted into expressions for the conductance either based on EMD or NEMD. As a MD based method, it not only includes anharmonicity, but also naturally includes the atomic level details of the interface quality. The ICMA method now enables more in-depth study of various effects such as temperature, anharmonicity, interdiffusion, roughness, imperfections, dislocations, stress, changes in crystal structure through a single unified model, as it can essentially treat any material or object where the atoms vibrate around equilibrium sites (e.g., ordered or disordered solids and molecules). This formalism therefore serves as an important step forward toward better understanding of heat flow at interfaces.

**Introduction**

When heat flows across an adjoining interface between two different materials there will be a temperature discontinuity at the interface. The interfacial heat flow can be written as the product of the interface conductance  $G$ , which is the inverse of the interfacial resistance, and the temperature difference across the interface  $\Delta T$ . The heat flow across the interface can be carried primarily by electrons in electrically conducting materials, but the contribution from the atomic motions is present in all materials. For solids and rigid molecules, these atomic motions correspond to vibrations around an equilibrium site, which can be decomposed into a series of eigen modes via the lattice dynamics (LD) formalism [1] where the actual anharmonic dynamics manifest as the modes having time varying amplitudes. At a given instant, by knowing the amplitudes of these eigen mode vibrations, one can sum the contributions of all the different eigen modes to recover the vibrations of each atom. The eigen modes are termed phonons in crystalline materials, since they generally correspond to propagating waves such as sound waves. However, in disordered/amorphous solids or molecules many eigen modes may not propagate or resemble the usual definition of a phonon. This has prompted our use of the term eigen mode in the ensuing discussion in order to retain generality, since the formalism presented herein is not restricted to crystalline solids.

Within the last decade, techniques have been developed to accurately calculate the individual eigen mode contributions to thermal conductivity from first principles [2–4]. These techniques now allow for predictive

calculations of the modal contributions to thermal conductivity for materials and nanostructures that have yet to be synthesized [5, 6]. Knowing the contributions of specific eigen modes can enable rational design and selection of materials by crafting certain features that will target certain group of modes (i.e., acoustic, optical, longitudinal or transverse), to either inhibit or enhance their transport [7–9]. This quantitative capability has improved our ability to predict classical size effects [10] and other nanoscale phenomena [11], which are important effects that ultimately limit heat dissipation in applications such as microelectronics [12]. As feature dimensions in micro/nanoelectronics continue to shrink, interfacial resistance is now much more important and in some cases can become the bottleneck to heat removal [13, 14]. Compared to the tremendous advancements in predicting thermal conductivity for crystalline materials over the last decade, predicting interface thermal conductance still faces many challenges. The central issue is that we lack quantitative understanding of the underlying processes that occur at interfaces, because we currently have no way of determining the modal contributions with full inclusion of anharmonicity.

Over the last 25 years, a variety of methods have been developed [15–21], but none of the methods that provide mode level details have fully included anharmonicity. Non-equilibrium molecular dynamics (NEMD) fully includes anharmonicity and has been used extensively to analyze different interface materials and interface qualities [22–26]. However, a formalism that can be used to study the modal contributions to  $G$  in the context of NEMD is lacking. As a result, the predictive power of methods that provide mode level details has been limited to low cryogenic temperatures, while most engineering applications involve temperatures above or near room temperature. Among the various methods that have been developed to investigate the modal contributions to  $G$  [15–18, 20, 21, 27], the most prominent are the acoustic mismatch model (AMM) [15, 16], the diffuse mismatch model (DMM) [17, 18, 28], the atomistic Green's function (AGF) approach [21, 27, 29–31], the harmonic LD based approaches [32–34], and the wave packet (WP) method [20, 35–37].

The AMM and DMM take the limit of purely specular and diffuse scattering respectively. Many improvements have been made to these methods [28, 38–42], but neither can include the atomic level detail of the interface quality (e.g., roughness, interatomic diffusion, stress, imperfections etc) and therefore they are fundamentally limited. The development of the AGF method was a major step forward, as it incorporated the atomic level details and also accounts for quantum effects [30, 43]. However, most applications of the AGF method have been limited to small system sizes and harmonic interactions, due to analytical complexity and computational expense [30]. Mingo nonetheless has shown that, in principle, anharmonicity can be included in the AGF [30]. To our knowledge, however, the anharmonic AGF has not yet been widely used. The WP method allows the calculation of a mode's transmissivity in the context of a MD simulation, however, it requires that all other modes have zero amplitude [30, 43–45]. This effectively corresponds to the  $T = 0$  K limit and therefore is unable to examine the effects of temperature dependent anharmonicity. As a result, the WP method simply reproduces the same results as the harmonic AGF approach [13].

Although exceptions exist [46], the majority of the literature associated with using the DMM has only been able to evaluate elastic scattering interactions where the transmission of a mode's energy across the interface is purely governed by whether or not other modes with similar frequency exist on the other side of the interface [13, 31]. It has been argued that inelastic scattering may not be important at room temperature, particularly in systems with nanoscale features [21], while others have argued that anharmonicity can have notable contributions to the thermal interface conductance at high temperatures [28, 44, 45, 47–49]. Until a method that includes anharmonicity/inelastic scattering is tested, it is difficult to conclude whether or not anharmonicity is important. The development and testing of such a method is the central focus of the ensuing discussion.

There have been two major breakthroughs over the past decade that have enabled our new approach. First, McGaughey and Kaviani [50, 51] showed that by projecting the instantaneous positions of the atoms in a molecular dynamics (MD) simulation onto the eigen mode solutions (i.e., the mode shapes from LD), one can calculate the instantaneous mode amplitudes as follows

$$X(\mathbf{k}, \nu) = \sum_{i=1}^N \frac{m_i^{1/2}}{N^{1/2}} \exp(-i\mathbf{k} \cdot \mathbf{r}_i) \mathbf{p}_i^* \cdot \mathbf{x}_i, \quad (1)$$

where  $\mathbf{k}$  is the wave vector,  $\nu$  is the mode frequency,  $\mathbf{p}_i$  is the polarization vector for atom  $i$ ,  $m_i$  is the mass for atom  $i$ ,  $\mathbf{r}_i$  is the equilibrium position for atom  $i$ ,  $\mathbf{x}_i$  is the displacement from the equilibrium for atom  $i$ ,  $*$  denotes the complex conjugate, and  $N$  is the total number of atoms. From the mode amplitude  $X$ , one can track the equilibrium fluctuations in the mode energy and can directly calculate the relaxation times of individual modes [50, 51]. This approach agrees with other independent methods and has contributed greatly to our ability to now calculate individual mode contributions to thermal conductivity from first principles [52–54]. The second major development that enabled our new formalism was introduced first by Barrat *et al* [55] and later by Domingues *et al* [56]. Both derived an expression for the conductance between any two groups of atoms, based on the fluctuation dissipation theorem. This approach has shown agreement with other methods such as NEMD [57] and now allows for calculation of thermal interface conductance without requiring an externally

applied heat flow. It is also important to note that the method introduced by Barrat *et al* [55] and Domingues *et al* [56] is general and can be applied to any phase of matter, where the atoms are simply divided into two groups such that the interface can have any arbitrary geometry or condition. Our new formalism introduced in the next section is termed the interface conductance modal analysis (ICMA) method as it combines the essential features of the modal decomposition method introduced by McGaughey and Kaviani [50, 51] with the equilibrium MD (EMD) conductance expression derived by Barrat *et al* [55] and Domingues *et al* [56]. With the ICMA method, we can determine the modal contributions to conductance at an interface and gauge the effects of anharmonicity/inelastic scattering as well as others (i.e., roughness, interdiffusion, stress, imperfections, dislocations etc) with fidelity.

## ICMA formalism

Suppose that we construct a system of two materials where each atom vibrates around an equilibrium site. The two materials can be labeled A and B and consist of  $N_A$  and  $N_B$  atoms respectively that can move in three-dimensions. When we bring these two systems into contact forming an interface, we can solve the equations of motion in the limit that the interactions are harmonic to obtain a set of  $3N = 3(N_A + N_B)$  eigen solutions via the LD formalism [1]. We can then write the atomic displacements and velocities as follows,

$$\mathbf{x}_i = \sum_n \frac{1}{(Nm_i)^{1/2}} \mathbf{e}_{n,i} X_n, \quad (2)$$

$$\dot{\mathbf{x}}_i = \sum_n \frac{1}{(Nm_i)^{1/2}} \mathbf{e}_{n,i} \dot{X}_n, \quad (3)$$

where the summations are over all the eigen modes  $n$  in the system,  $\mathbf{x}_i$ ,  $\dot{\mathbf{x}}_i$ ,  $m_i$  are the displacement from equilibrium, velocity and mass of atom  $i$  respectively, and  $\mathbf{e}_{n,i}$  is the vector (containing 3 Cartesian components) associated with atom  $i$  that is contained within the  $3N \times 1$  eigen vector matrix that represents the  $n$ th solution to the equations of motion. The vector  $\mathbf{e}_{n,i}$  specifies the direction and magnitude of vibration attributed to the atom  $i$  as it participates in the collective motion associated with mode  $n$ .  $X_n$  and  $\dot{X}_n$  are the normal mode coordinates for the position and velocity of mode  $n$ , which can be calculated from the inverse of the operations in equations (2) and (3) as

$$X_n = \sum_i \frac{m_i^{1/2}}{N^{1/2}} \mathbf{x}_i \cdot \mathbf{e}_{n,i}^*, \quad (4)$$

$$\dot{X}_n = \sum_i \frac{m_i^{1/2}}{N^{1/2}} \dot{\mathbf{x}}_i \cdot \mathbf{e}_{n,i}^*, \quad (5)$$

where the summations are over all the atoms  $i$  in the system and  $*$  denotes complex conjugate. For crystalline materials, where there is long range order and periodicity, the eigen vectors  $\mathbf{e}_{n,i}$  are usually expressed in terms of a wave vector  $\mathbf{k}$  and branch  $\nu$  in the dispersion diagram as follows

$$\mathbf{e}_{n,i} = \exp(\mathbf{i}\mathbf{k} \cdot \mathbf{r}_{i,0}) \mathbf{e}_i(\mathbf{k}_\nu), \quad (6)$$

where  $\mathbf{r}_{i,0}$  is the equilibrium position, and  $\mathbf{e}_i(\mathbf{k}_\nu)$  is the eigen mode displacement for atom  $i$ . This is the more common definition, which is consistent with equation (1). Here, however, we have used a single index  $n$  as a label for the eigen solutions instead of the wave vector  $\mathbf{k}$  and polarization/frequency to identify each mode. This is done to retain generality, since it is not required that the system exhibit long range order/periodicity and therefore not all modes have to correspond to propagating wave solutions.

Following the approach pioneered by Barrat *et al* [55] and Domingues *et al* [56], we can write the instantaneous heat flow across the interface by simply grouping the atoms into two groups, namely A and B. At each instant, in a microcanonical ensemble, the rate at which energy is transmitted across the boundaries of material A is equal to the instantaneous rate of change of the energy in material B. The Hamiltonian of a system having  $N$  atoms can be written as

$$H = \sum_i \frac{\mathbf{p}_i^2}{2m_i} + \Phi(\mathbf{r}_1, \mathbf{r}_2, \dots, \mathbf{r}_N), \quad (7)$$

where  $\mathbf{r}_i$  and  $\mathbf{p}_i$  represent the position and momentum of atom  $i$ , respectively, and  $\Phi$  represents the total potential energy of the system. The individual Hamiltonian for atom  $i$  can then be written as

$$H_i = \frac{\mathbf{p}_i^2}{2m_i} + \Phi_i(\mathbf{r}_1, \mathbf{r}_2, \dots, \mathbf{r}_n), \quad (8)$$

where  $\Phi_i$  is the potential energy associated with a single atom [52, 58]. Using this definition for an individual atom's Hamiltonian, the instantaneous energy exchanged between material A and B is given by

$$Q_{A \rightarrow B} = -\sum_{i \in A} \sum_{j \in B} \left\{ \frac{p_{i,\alpha}}{m_i} \left( \frac{-\partial H_j}{\partial \mathbf{r}_i} \right) + \frac{p_{j,\alpha}}{m_j} \left( \frac{\partial H_i}{\partial \mathbf{r}_j} \right) \right\}. \quad (9)$$

Equation (9) is general and can be applied to any model for the atomic interactions that can be represented as a sum of individual atom energies. If only pairwise interactions are present between material A and B, equation (9) can be reduced to

$$Q_{A \rightarrow B} = -\frac{1}{2} \sum_{i \in A} \sum_{j \in B} \mathbf{f}_{ij} \cdot (\dot{\mathbf{x}}_i + \dot{\mathbf{x}}_j), \quad (10)$$

where  $\mathbf{f}_{ij}$  is the pairwise interaction force between the two materials [48, 56, 59]. For pairwise interactions, it is a natural choice to partition half of the energy in the interaction with atom  $i$  and the other half with atom  $j$ . From this relation, Domingues *et al* [56] used the fluctuation-dissipation theorem to show that the correlation in the equilibrium fluctuations of the heat flow are related to the conductance via

$$G = \frac{1}{Ak_B T^2} \int_0^\infty \langle Q_{A \rightarrow B}(t) \cdot Q_{A \rightarrow B}(0) \rangle dt, \quad (11)$$

where  $G$  is the thermal conductance between the two materials,  $A$  is the interface contact area,  $k_B$  is the Boltzmann constant,  $T$  is the equilibrium temperature of the system, and  $\langle \dots \rangle$  represents the autocorrelation function. This result is in principle similar to the more widely used Green–Kubo expression for thermal conductivity calculations [52]. To simplify the nomenclature, we will use  $Q$  instead of  $Q_{A \rightarrow B}$  for interfacial heat flow in the ensuing discussion.

It follows from equation (11) that if one could obtain the modal contributions to the heat flow across the interface, such that, at every instant the sum of those contributions returned the total  $Q$ ,

$$Q = \sum_n Q_n \quad (12)$$

then  $G$  can be rewritten as

$$G = \frac{1}{Ak_B T^2} \int \left\langle \sum_n Q_n(t) \cdot Q(0) \right\rangle dt = \sum_n \frac{1}{Ak_B T^2} \int \langle Q_n(t) \cdot Q(0) \rangle dt. \quad (13)$$

This would then give the individual contribution of each mode to  $G$  as

$$G_n = \frac{1}{Ak_B T^2} \int \langle Q_n(t) \cdot Q(0) \rangle dt, \quad (14)$$

where

$$G = \sum_n G_n. \quad (15)$$

Moreover, the definition of the modal heat flux in equation (12) would allow us to substitute for the total heat flux in both places in equation (11) yielding another expression for  $G$  as,

$$G = \frac{1}{Ak_B T^2} \int \left\langle \sum_n Q_n(t) \cdot \sum_{n'} Q_{n'}(t) \right\rangle dt = \sum_n \sum_{n'} \frac{1}{Ak_B T^2} \int \langle Q_n(t) \cdot Q_{n'}(0) \rangle dt \quad (16)$$

with individual contributions from correlations between pairs of modes equal to,

$$G_{n,n'} = \frac{1}{Ak_B T^2} \int \langle Q_n(t) \cdot Q_{n'}(0) \rangle dt. \quad (17)$$

This format expresses the interface conductance as the summation of all the auto-correlations and cross-correlations between eigen mode pairs  $n$  and  $n'$  in the system ( $G = \sum_{n,n'} G_{n,n'}$ ) and would provide new insight into which modes interact. This insight into the mode-mode interactions by ICMA may in some ways be related to the recent elucidation of interfacial scattering interactions using the non-equilibrium Green's function (NEGF) method by Ong and Zhang [60]. However, their application of the NEGF approach did not include anharmonicity and as a result, the ICMA method provides additional detail and potentially deeper insights into the physics than purely harmonic approaches.

The critical step is then to determine  $Q_n$ , subject to the requirement that  $Q = \sum_n Q_n$ . This can be done by replacing the velocity of each atom in equation (9) with the sum of modal contributions in equation (3),

$$\begin{aligned}
Q &= \sum_{i \in A} \sum_{j \in B} \left\{ \left( \sum_n \frac{1}{(Nm_i)^{1/2}} \mathbf{e}_{n,i} \dot{X}_n \right) \cdot \left( \frac{\partial H_j}{\partial \mathbf{r}_i} \right) - \left( \sum_n \frac{1}{(Nm_j)^{1/2}} \mathbf{e}_{n,j} \dot{X}_n \right) \cdot \left( \frac{\partial H_i}{\partial \mathbf{r}_j} \right) \right\} \\
Q_n &= \frac{1}{N^{1/2}} \sum_{i \in A} \sum_{j \in B} \left\{ \left( \frac{1}{(m_i)^{1/2}} \mathbf{e}_{n,i} \dot{X}_n \right) \cdot \left( \frac{\partial H_j}{\partial \mathbf{r}_i} \right) + \left( \frac{1}{(m_j)^{1/2}} \mathbf{e}_{n,j} \dot{X}_n \right) \cdot \left( \frac{-\partial H_i}{\partial \mathbf{r}_j} \right) \right\}. \quad (18)
\end{aligned}$$

Equation (18) is general and for pairwise interactions it simplifies to,

$$Q_n = \sum_{i \in A} \sum_{j \in B} \frac{-\mathbf{f}_{ij}}{2} \cdot \left( \frac{1}{(Nm_i)^{1/2}} \mathbf{e}_{n,i} \dot{X}_n + \frac{1}{(Nm_j)^{1/2}} \mathbf{e}_{n,j} \dot{X}_n \right). \quad (19)$$

In using the substitution of the modal contributions to velocity (equation (3)), we postulate that any quantity that is a direct function of the atomic displacements and/or velocities can be decomposed into its modal contributions via equations (2) and (3). This includes quantities such as temperature [61], pressure [62], entropy [63], heat capacity [64], etc. The issue with equation (9), however, is that it includes the vibrations from both sides of the interface. Using such an expression is inconsistent with the prevailing paradigm used to understand heat flow at solid interfaces, which is based on the phonon gas model (PGM) and the Landauer formalism [65]. The inconsistency arises from the fact that in Landauer formalism although the transmission probabilities are calculated based on the interaction of the atoms at the two sides of interface, the final summation, as a consequence of the principle of detailed balance, however, is only cast in terms of the modes on one side of the interface, where the net heat flow is written as [28, 65],

$$q = \sum_{p_A} \left[ \frac{1}{V_A} \sum_{k_{x,A}=-k_{\max}}^{k_{\max}} \sum_{k_{y,A}=-k_{\max}}^{k_{\max}} \sum_{k_{z,A}=0}^{k_{\max}} v_{z,A} \hbar \omega \tau_{AB} \times \left( f(\omega, T_A) - f(\omega, T_B) \right) \right]. \quad (20)$$

In equation (20) the summations are over different polarizations ( $p$ ) and allowed wave vectors ( $k_{x,y,z}$ ) in either material A or B [65]. Here, it is critically important to recognize that current understanding of interfacial heat flow has been, in essence, entirely based on using the modes of an isolated bulk crystal. However, since the modes of an isolated bulk crystal do not involve the atoms of the other material that forms the interface, an expression for the interfacial heat flow that uses the velocities of both sides is conceptually inconsistent with the prevailing view of interfacial transport. Equation (20) is therefore inconsistent with equations (9) and (10), because one cannot project the vibrations of atoms from side B onto the modes of side A or vice versa. Such an operation is ill defined if only the modes associated with one side are used to describe the heat flow. In this sense, the fact that the velocities from both sides of the interface manifest in equation (9), raises interesting questions around whether or not a different set of vibrational modes should be used for describing interfacial heat flow; particularly since previous work has shown that the vibrations of the atoms near an interface can exhibit distinctly different frequency content than the rest of the bulk material [22, 66]. For this reason, we perform a LD calculation on the entire combined system, so that equation (18) can be used directly without modification.

It is important to note that positive conductance is not strictly guaranteed by equation (11). Nonetheless, cases of negative conductance have not been observed, as negative thermal conductivity or negative conductance would violate the second law of thermodynamics. It should also be noted, however, that negative conductance contributions from individual modes are not prohibited by this formalism, as it is possible that the integral of the cross-correlations between a mode and all others could be more negative than the auto-correlation is positive. Consequently, in this formalism an individual mode can exhibit a negative conductance contribution. However, because the total conductance is positive in practice, such an occurrence does not violate the second law. Negative conductance contributions, on the other hand, are still inconsistent with the PGM. The PGM, however, is not a fundamental law, rather it is an accurate model for treating phonon-phonon interactions in crystalline bulk materials that has been widely used. There are other classes of materials, such as disordered materials (i.e., alloys and amorphous materials), where the validity of the PGM is questionable and the formalism presented herein merely offers a different and arguably more general viewpoint that does not require the definition of phonon velocities. As a result one can expect to observe negative contributions to the conductance from individual modes, but overall positive conductance from the entire system of modes, in accordance with the second law. It should also be noted that similar to any other property calculated with MD simulations (i.e., thermal conductivity [67]), the values of interface thermal conductance predicted by this formalism will depend on the interatomic potential used. This issue, however, does not affect the generality of the ICMA formalism as the interface conductance can in principle be calculated *ab initio*. Here, one could

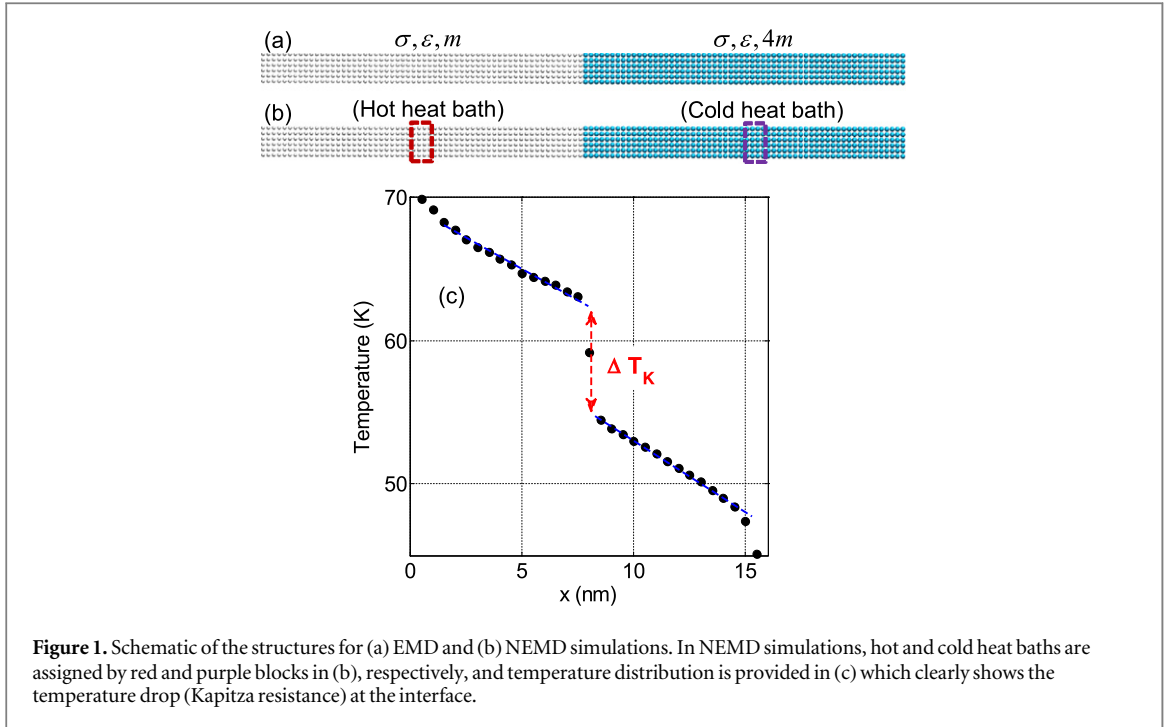


**Figure 1.** Schematic of the structures for (a) EMD and (b) NEMD simulations. In NEMD simulations, hot and cold heat baths are assigned by red and purple blocks in (b), respectively, and temperature distribution is provided in (c) which clearly shows the temperature drop (Kapitza resistance) at the interface.

construct an accurate interatomic potential as a Taylor expansion of the energy with respect to the atom displacements as has been demonstrated by Esfarjani *et al* using the direct displacement method [68].

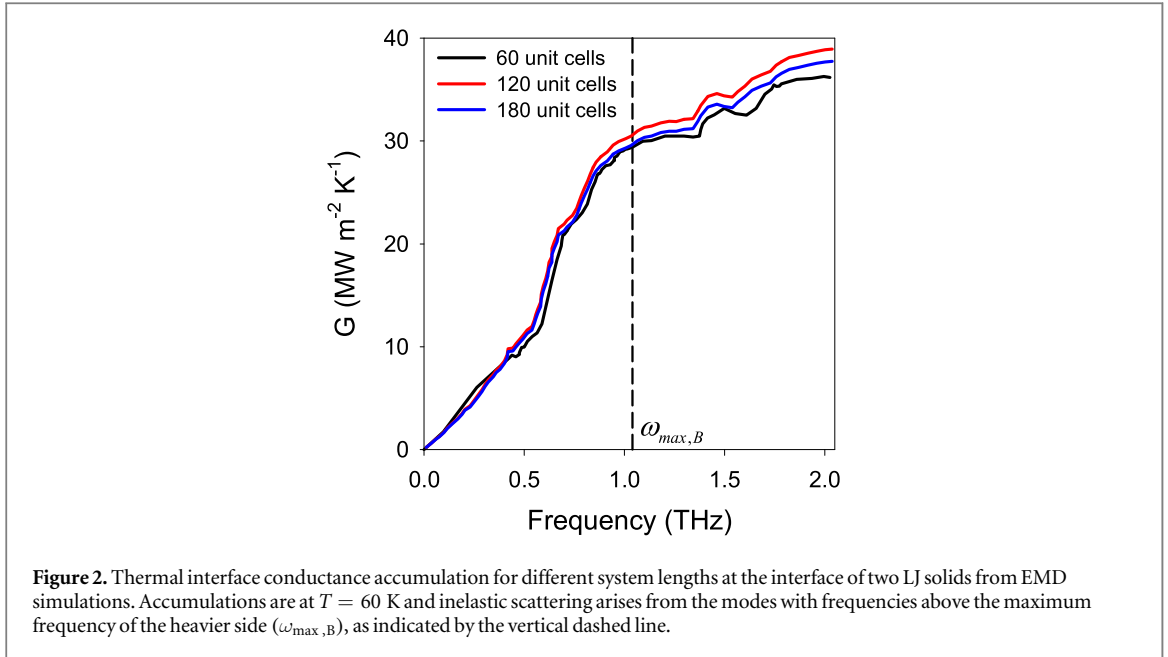
## Simulation methodology

As an initial application of the ICMA method, we studied a simple interface between Lennard-Jones (LJ) crystals. The LJ potential is defined based on the following formula [69]:

$$\Phi = 4\epsilon \left[ \left( \frac{\sigma}{r} \right)^{12} - \left( \frac{\sigma}{r} \right)^6 \right]. \quad (21)$$

We select equal values of  $\epsilon$  and  $\sigma$  for both materials A and B, which results in equal lattice constants for the two sides. An acoustic mismatch exists at the interface because the mass of the atoms on side B are four times the mass of atoms on side A ( $m_B = 4m_A$ ). Both sides have face-centered-cubic (FCC) lattice structures. In LJ systems the simulations can be performed in LJ dimensionless units [57], but to have the results correspond to a physically meaningful system, we chose LJ parameters in our simulations to be equal to that of argon ( $\epsilon = 1.67 \times 10^{-21}$  J,  $\sigma = 3.405$  Å, and  $m_A = 6.6 \times 10^{-26}$  kg [70]). Thus, side A represents solid argon (mass  $m$ ) and side B represents a fictitiously heavier solid argon (mass  $4m$ ). In our EMD simulations, the system consists of  $3 \times 3 \times 60$  fcc unit cells (each side 30 unit cells long), which includes 2160 atoms and 6480 eigen modes. A schematic of the structure can be seen in figure 1(a). We confirmed that increasing the size of cross section does not change the features observed in the results, which is in agreement with other reports [31, 59]. We also checked the effect of system size on the calculated modal contributions, which is presented in the results section (figure 2), which shows that increasing the length of the system has a negligible impact on the general trend of the calculated modal contributions. Initially, the system is simulated for 2 ns to reach equilibrium. Then, modal heat flux contributions ( $Q_n$ ) are recorded for 5 ns in the micro-canonical ensemble. The modal contributions to the heat flow,  $Q_n$ , are then used in post processing (see equation (14)), which leads to the calculation of modal thermal conductance ( $G_n$ ). Examples of calculated correlation functions and the respective evolution of interface thermal conductance are shown in figures S1 in the supplementary materials.

The modal heat flux in equation (19) can also be readily used in NEMD simulations to obtain modal contributions to interface conductance. Here we used  $G = \frac{\bar{Q}}{\Delta T}$ , where  $\bar{Q}$  is the time-averaged heat flux in the NEMD simulation, and  $\Delta T$  is the temperature difference at the interface, determined by extrapolation of the temperature gradients in each respective material [23, 71–73]. The modal contribution to the conductance ( $G_n$ ) then becomes



$$G_n = \frac{\overline{Q_n}}{\Delta T}, \quad (22)$$

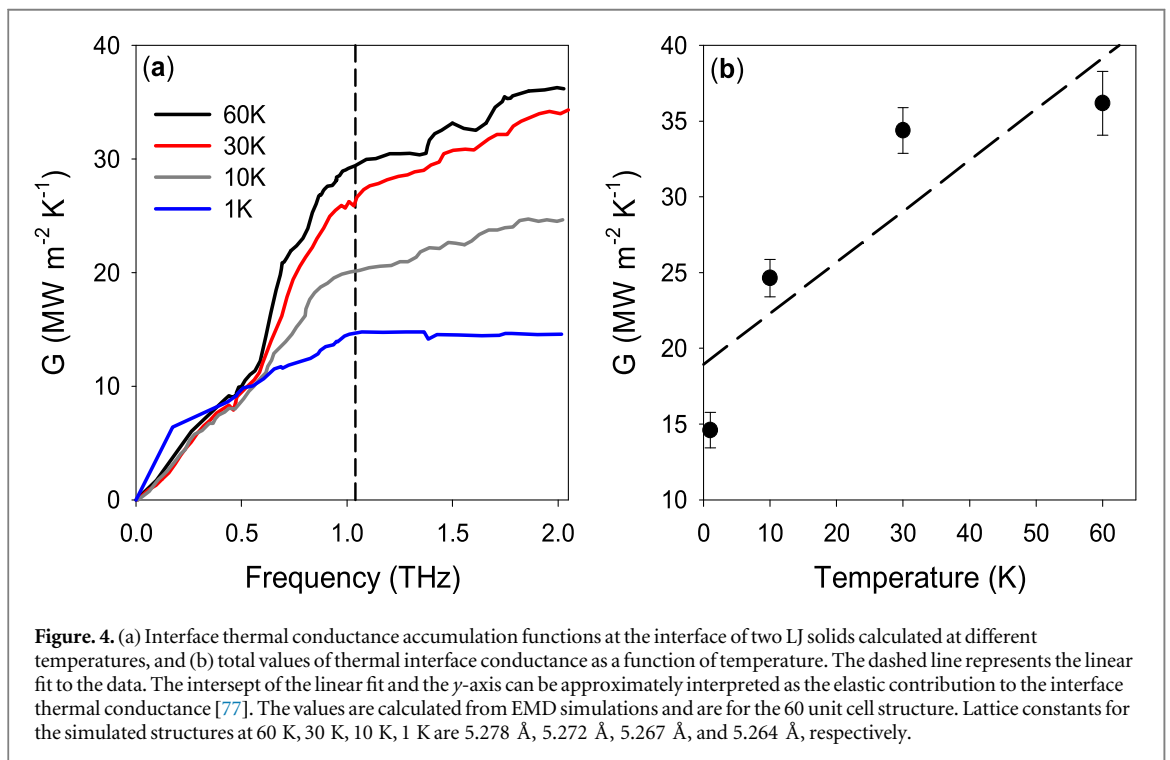
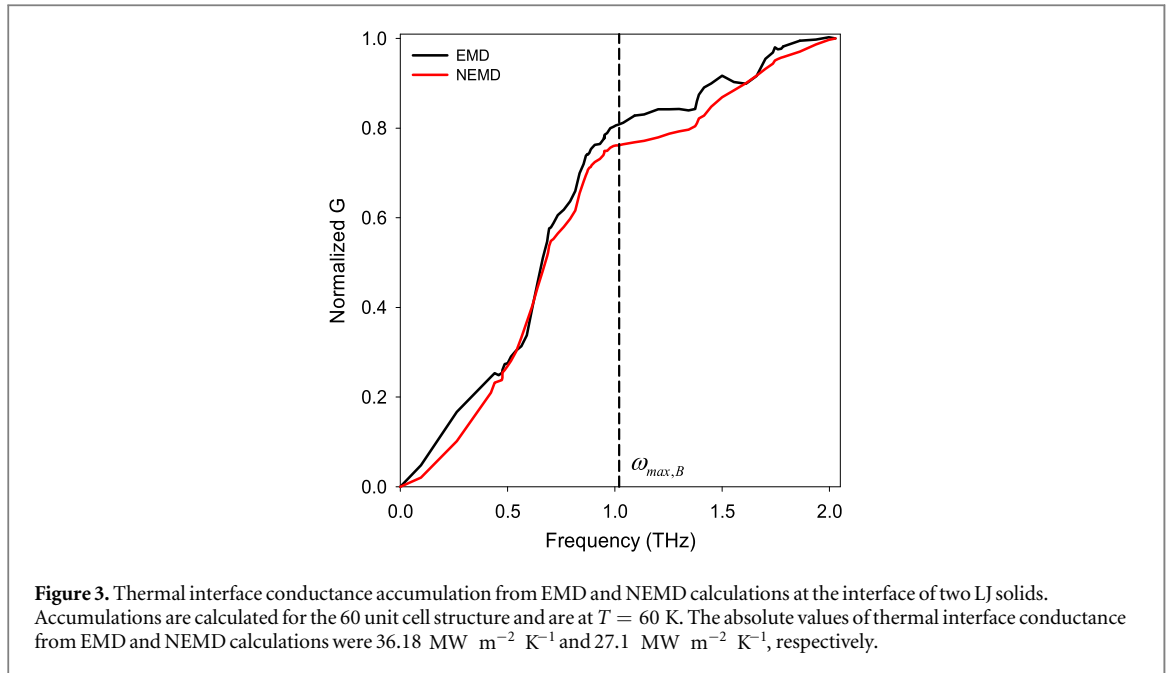
where the same  $\Delta T$  is used for every mode. We used periodic boundary conditions along all Cartesian directions. Hot and cold heat baths were placed in the middle of the left side (mass  $m$ ) and right side (mass  $4m$ ) of the interface, respectively (see figure 1(b)). A thermal power equal to 6.5 nW is input to the system from the hot bath and extracted from the system from the cold bath. The system is simulated for 2 ns to reach steady state, after which the temperature profile remains constant throughout the structure, which can be seen in figure 1(c). We then averaged the modal heat flux contributions for 2 ns and used equation (22) to calculate the modal contributions to the interface conductance of the interface of two LJ materials. For both EMD and NEMD simulations a time step of 1 fs was considered and the standard deviation in  $G$  was less than 5% for five independent initial conditions [74].

## Results and discussion

For this system, using EMD simulations, we calculated the thermal interface conductance accumulation function for three different system lengths, which is shown in figure 2. The results show that choosing different lengths for the structure does not change the calculated modal contributions to interface thermal conductance (e.g., <6%). In figure 2 we also identify the frequency above which the heavier side does not have any modes available that can be supported in the bulk of the material. Above this frequency, all of the conductance can be attributed to inelastic/anharmonic processes, since purely harmonic interactions would cause the accumulation to reach 100% by  $\omega_{\max,B}$ . Thermal interface conductance accumulation functions for the LJ interface obtained from NEMD simulations are also shown in figure 3 compared with the EMD result. Although small differences exist, the result shows that ICMA yields a similar trend in the normalized modal contributions between EMD and NEMD approaches. Here, we have used normalized thermal interface conductance accumulations to compare EMD and NEMD approaches, because for this case the total values of conductance differ for the two approaches, as has been observed previously [75, 76].

The effect of temperature on the calculated modal contributions to thermal interface conductance from EMD simulations is also presented in figure 4. The observed decrease in the values of total thermal interface conductance as the temperature decreases is similar to the trend reported by Duda *et al* [77].

The temperature dependent calculations presented in figure 4 clearly show the importance of anharmonicity. Unlike thermal conductivity in crystals, which is well known to decrease due to anharmonicity, at interfaces, anharmonicity opens up channels for heat conduction, by allowing modes with different frequencies to interact. This has the net effect of increasing the conductance in this system, which is evidenced by the higher conductance values at higher temperatures and more specifically the increased contribution to the total conductance from modes with frequencies above  $\omega_{\max,B}$ .



## Conclusions

A new approach, termed the ICMA method has been presented, which allows one to calculate the modal contributions to thermal interface conductance. The approach is based on the modal decomposition of the instantaneous heat flow across an interface, which can be implemented in either EMD or NEMD simulations. Results from both EMD and NEMD simulations of a LJ solid interface with ICMA show agreement for the normalized thermal interface conductance accumulation versus frequency. This new formalism provides an alternative and arguably more complete picture of the modal contributions to conductance at interfaces since it includes anharmonicity to full order. Many additional comparative studies to understand the effects of temperature, anharmonicity, interdiffusion, roughness, imperfections, dislocations, stress, changes in crystal structure etc are needed. The new ICMA formalism presented herein serves as a critical step forward, which now

enables a high degree of fidelity in studying such effects and is expected to lead to even more new insights on how to rationally design and select materials for applications involving heat flow across interfaces.

## Acknowledgments

We acknowledge useful discussions with Professor Michael Leamy.

## References

- [1] Dove M T 1993 *Introduction to Lattice Dynamics* vol 4 (Cambridge: Cambridge University Press)
- [2] Broido D, Malorny M, Birner G, Mingo N and Stewart D 2007 Intrinsic lattice thermal conductivity of semiconductors from first principles *Appl. Phys. Lett.* **91** 231922
- [3] Jain A and McGaughey A J 2015 Strongly anisotropic in-plane thermal transport in single-layer black phosphorene *Sci. Rep.* **5** 8501
- [4] Garg J, Bonini N, Kozinsky B and Marzari N 2011 Role of disorder and anharmonicity in the thermal conductivity of silicon-germanium alloys: a first-principles study *Phys. Rev. Lett.* **106** 045901
- [5] Dresselhaus M *et al* 2009 New composite thermoelectric materials for energy harvesting applications *JOM* **61** 86–90
- [6] Lindsay L, Broido D and Reinecke T 2013 First-principles determination of ultrahigh thermal conductivity of boron arsenide: a competitor for diamond? *Phys. Rev. Lett.* **111** 025901
- [7] Shen S, Henry A, Tong J, Zheng R and Chen G 2010 Polyethylene nanofibres with very high thermal conductivities *Nat. Nanotechnology* **5** 251–5
- [8] Dresselhaus M S *et al* 2007 New directions for low-dimensional thermoelectric materials *Adv. Mater.* **19** 1043–53
- [9] Yang R, Chen G and Dresselhaus M S 2005 Thermal conductivity of simple and tubular nanowire composites in the longitudinal direction *Phys. Rev. B* **72** 125418
- [10] Li D *et al* 2003 Thermal conductivity of individual silicon nanowires *Appl. Phys. Lett.* **83** 2934–6
- [11] Yang R and Chen G 2004 Thermal conductivity modeling of periodic two-dimensional nanocomposites *Phys. Rev. B* **69** 195316
- [12] Pop E 2010 Energy dissipation and transport in nanoscale devices *Nano Res.* **3** 147–69
- [13] Cahill D G *et al* 2014 Nanoscale thermal transport: II. 2003–2012 *Appl. Phys. Rev.* **1** 011305
- [14] Cahill D G *et al* 2002 Nanoscale thermal transport *J. Appl. Phys.* **93** 793–818
- [15] Khalatnikov I M 1952 Teploobmen mezhdru tverdyim telom I geliem-Ii 1952 *Zh. Eksp. Teor. Fiz.* **22** 687–704
- [16] Little W 1959 The transport of heat between dissimilar solids at low temperatures *Can. J. Phys.* **37** 334–49
- [17] Swartz E and Pohl R 1987 Thermal resistance at interfaces *Appl. Phys. Lett.* **51** 2200–2
- [18] Swartz E T and Pohl R O 1989 Thermal boundary resistance *Rev. Mod. Phys.* **61** 605
- [19] Mingo N 2003 Calculation of Si nanowire thermal conductivity using complete phonon dispersion relations *Phys. Rev. B* **68** 113308
- [20] Schelling P, Phillpot S and Keblinski P 2004 Kapitza conductance and phonon scattering at grain boundaries by simulation *J. Appl. Phys.* **95** 6082–91
- [21] Zhang W, Fisher T and Mingo N 2007 The atomistic Green's function method: an efficient simulation approach for nanoscale phonon transport *Numer. Heat Transfer B* **51** 333–49
- [22] English T S *et al* 2012 Enhancing and tuning phonon transport at vibrationally mismatched solid-solid interfaces *Phys. Rev. B* **85** 035438
- [23] Gordiz K and Allaei S M V 2014 Thermal rectification in pristine-hydrogenated carbon nanotube junction: a molecular dynamics study *J. Appl. Phys.* **115** 163512
- [24] Landry E and McGaughey A 2009 Thermal boundary resistance predictions from molecular dynamics simulations and theoretical calculations *Phys. Rev. B* **80** 165304
- [25] Luo T and Lloyd J R 2012 Enhancement of thermal energy transport across graphene/graphite and polymer interfaces: a molecular dynamics study *Adv. Funct. Mater.* **22** 2495–502
- [26] Zhong H L and Lukes J R 2006 Interfacial thermal resistance between carbon nanotubes: molecular dynamics simulations and analytical thermal modeling *Phys. Rev. B* **74** 125403
- [27] Mingo N and Yang L 2003 Phonon transport in nanowires coated with an amorphous material: an atomistic Green's function approach *Phys. Rev. B* **68** 245406
- [28] Hopkins P E, Norris P M and Duda J C 2011 Anharmonic phonon interactions at interfaces and contributions to thermal boundary conductance *J. Heat Transfer* **133** 062401
- [29] Zhang W, Mingo N and Fisher T 2007 Simulation of interfacial phonon transport in Si–Ge heterostructures using an atomistic Green's function method *J. Heat Transfer* **129** 483–91
- [30] Mingo N 2009 *Thermal Nanosystems and Nanomaterials* (Berlin: Springer) pp 63–94
- [31] Tian Z, Esfarjani K and Chen G 2012 Enhancing phonon transmission across a Si/Ge interface by atomic roughness: first-principles study with the Green's function method *Phys. Rev. B* **86** 235304
- [32] Young D and Maris H 1989 Lattice-dynamical calculation of the Kapitza resistance between fcc lattices *Phys. Rev. B* **40** 3685
- [33] Sun H and Pipe K P 2012 Perturbation analysis of acoustic wave scattering at rough solid–solid interfaces *J. Appl. Phys.* **111** 023510
- [34] Zhao H and Freund J B 2009 Phonon scattering at a rough interface between two fcc lattices *J. Appl. Phys.* **105** 013515
- [35] Baker C H, Jordan D A and Norris P M 2012 Application of the wavelet transform to nanoscale thermal transport *Phys. Rev. B* **86** 104306
- [36] Schelling P K, Phillpot S R and Keblinski P 2002 Phonon wave-packet dynamics at semiconductor interfaces by molecular-dynamics simulation *Appl. Phys. Lett.* **80** 2484–6
- [37] Roberts N A and Walker D 2010 Phonon wave-packet simulations of Ar/Kr interfaces for thermal rectification *J. Appl. Phys.* **108** 123515
- [38] Hopkins P E 2009 Multiple phonon processes contributing to inelastic scattering during thermal boundary conductance at solid interfaces *J. Appl. Phys.* **106** 013528
- [39] Hopkins P E and Norris P M 2007 Effects of joint vibrational states on thermal boundary conductance *Nanoscale Microscale Thermophys. Eng.* **11** 247–57
- [40] Prasher R 2009 Acoustic mismatch model for thermal contact resistance of van der Waals contacts *Appl. Phys. Lett.* **94** 041905

- [41] Reddy P, Castelino K and Majumdar A 2005 Diffuse mismatch model of thermal boundary conductance using exact phonon dispersion *Appl. Phys. Lett.* **87** 211908
- [42] Shin S, Kaviany M, Desai T and Bonner R 2010 Roles of atomic restructuring in interfacial phonon transport *Phys. Rev. B* **82** 081302
- [43] Minnich A J 2015 Advances in the measurement and computation of thermal phonon transport properties *J. Phys.: Condens. Matter* **27** 053202
- [44] Stevens R J, Zhigilei L V and Norris P M 2007 Effects of temperature and disorder on thermal boundary conductance at solid–solid interfaces: nonequilibrium molecular dynamics simulations *Int. J. Heat Mass Transfer* **50** 3977–89
- [45] Hopkins P E, Stevens R J and Norris P M 2008 Influence of inelastic scattering at metal–dielectric interfaces *J. Heat Transfer* **130** 022401
- [46] Duda J C, Beechem T E, Smoyer J L, Norris P M and Hopkins P E 2010 Role of dispersion on phononic thermal boundary conductance *J. Appl. Phys.* **108** 073515
- [47] Chalopin Y and Volz S 2013 A microscopic formulation of the phonon transmission at the nanoscale *Appl. Phys. Lett.* **103** 051602
- [48] Ong Z-Y and Pop E 2010 Frequency and polarization dependence of thermal coupling between carbon nanotubes and SiO<sub>2</sub> *J. Appl. Phys.* **108** 103502
- [49] Chalopin Y, Mingo N, Diao J, Srivastava D and Volz S 2012 Large effects of pressure induced inelastic channels on interface thermal conductance *Appl. Phys. Lett.* **101** 221903
- [50] McGaughey A J and Kaviany M 2004 Quantitative validation of the Boltzmann transport equation phonon thermal conductivity model under the single-mode relaxation time approximation *Phys. Rev. B* **69** 094303
- [51] McGaughey A and Kaviany M 2004 Thermal conductivity decomposition and analysis using molecular dynamics simulations: I. Lennard-Jones argon *Int. J. Heat Mass Transfer* **47** 1783–98
- [52] Henry A S and Chen G 2008 Spectral phonon transport properties of silicon based on molecular dynamics simulations and lattice dynamics *J. Comput. Theor. Nanosci.* **5** 141–52
- [53] Henry A and Chen G 2008 High thermal conductivity of single polyethylene chains using molecular dynamics simulations *Phys. Rev. Lett.* **101** 235502
- [54] Henry A and Chen G 2009 Anomalous heat conduction in polyethylene chains: theory and molecular dynamics simulations *Phys. Rev. B* **79** 144305
- [55] Barrat J-L and Chiaruttini F 2003 Kapitza resistance at the liquid–solid interface *Mol. Phys.* **101** 1605–10
- [56] Domingues G, Volz S, Joulain K and Greffet J-J 2005 Heat transfer between two nanoparticles through near field interaction *Phys. Rev. Lett.* **94** 085901
- [57] Rajabpour A and Volz S 2010 Thermal boundary resistance from mode energy relaxation times: case study of argon-like crystals by molecular dynamics *J. Appl. Phys.* **108** 094324
- [58] Hardy R J 1963 Energy-flux operator for a lattice *Phys. Rev.* **132** 168
- [59] Chalopin Y, Esfarjani K, Henry A, Volz S and Chen G 2012 Thermal interface conductance in Si/Ge superlattices by equilibrium molecular dynamics *Phys. Rev. B* **85** 195302
- [60] Ong Z-Y and Zhang G 2015 Efficient approach for modeling phonon transmission probability in nanoscale interfacial thermal transport *Phys. Rev. B* **91** 174302
- [61] Shiomi J and Maruyama S 2006 Non-fourier heat conduction in a single-walled carbon nanotube: classical molecular dynamics simulations *Phys. Rev. B* **73** 205420
- [62] Mori Y and Okumura H 2014 High pressure effect on a helical peptide studied by simulated tempering molecular dynamics simulations *Biophys. J.* **106** 611a
- [63] Lin S-T, Maiti P K and Goddard W A III 2010 Two-phase thermodynamic model for efficient and accurate absolute entropy of water from molecular dynamics simulations *J. Phys. Chem. B* **114** 8191–8
- [64] Rajabpour A, Akizi F Y, Heyhat M M and Gordiz K 2013 Molecular dynamics simulation of the specific heat capacity of water–Cu nanofluids *Int. Nano Lett.* **3** 58
- [65] Chen G 2005 *Nanoscale Energy Transport and Conversion: A Parallel Treatment of Electrons, Molecules, Phonons, and Photons* (New York: Oxford University Press)
- [66] Yang N *et al* 2015 Thermal interface conductance between aluminum and silicon by molecular dynamics simulations *J. Comput. Theor. Nanosci.* **12.2** 168–74
- [67] Lukes J R and Zhong H 2007 Thermal conductivity of individual single-wall carbon nanotubes *J. Heat Transfer* **129** 705–16
- [68] Esfarjani K, Chen G and Stokes H T 2011 Heat transport in silicon from first-principles calculations *Phys. Rev. B* **84** 085204
- [69] Rafii-Tabar H 2008 *Computational Physics of Carbon Nanotubes* (Cambridge: Cambridge University Press)
- [70] Sarkar S and Selvam R P 2007 Molecular dynamics simulation of effective thermal conductivity and study of enhanced thermal transport mechanism in nanofluids *J. Appl. Phys.* **102** 074302
- [71] Wu X and Luo T 2014 The importance of anharmonicity in thermal transport across solid–solid interfaces *J. Appl. Phys.* **115** 014901
- [72] Rajabpour A, Allaei S V and Kowsary F 2011 Interface thermal resistance and thermal rectification in hybrid graphene-graphane nanoribbons: a nonequilibrium molecular dynamics study *Appl. Phys. Lett.* **99** 051917
- [73] Hu M, Keblinski P and Schelling P K 2009 Kapitza conductance of silicon–amorphous polyethylene interfaces by molecular dynamics simulations *Phys. Rev. B* **79** 104305
- [74] Gordiz K, Singh D J and Henry A 2015 Ensemble averaging versus time averaging in molecular dynamics simulations of thermal conductivity *J. Appl. Phys.* **117** 045104
- [75] Shen M, Schelling P K and Keblinski P 2013 Heat transfer mechanism across few-layer graphene by molecular dynamics *Phys. Rev. B* **88** 045444
- [76] Murakami T, Hori T, Shiga T and Shiomi J 2014 Probing and tuning inelastic phonon conductance across finite-thickness interface *Appl. Phys. Express* **7** 121801
- [77] Duda J C *et al* 2011 Implications of cross-species interactions on the temperature dependence of Kapitza conductance *Phys. Rev. B* **84** 193301